DOI:10.1021/jf9016288

JOURNAL OF AGRICULTURAL AND FOOD CHEMISTRY
ARTICLE

Detection and Isolation of Antiatherogenic and Antioxidant Substances Present in Olive Mill Wastes by a Novel Filtration System

George Stamatakis,[†] Nektaria Tsantila,[†] Martina Samiotaki,[‡] George N. Panayotou,[‡] Alexandros C. Dimopoulos,[§] Constantinos P. Halvadakis,[∥] and Constantinos A. Demopoulos*,[†]

[†]Faculty of Chemistry, National and Kapodistrian University of Athens, Athens, Greece, [‡]Protein Chemistry Laboratory BSRC "Alexander Fleming", Vari, Athens, Greece, [§]School of Electrical and Computer Engineering, National Technical University of Athens, Athens, Greece, and [∥]Department of Environment, University of the Aegean, Mytilene, Greece

Olive mill waste water (OMWW) is a major environmental issue in the Mediterranean. We address this problem by investigating the wastes for the presence of biologically active compounds already detected in both olive oil and pomace. Two initial OMWW samples were filtered using two microporous filtering media: (a) clayey diatomite and (b) zeolitic volcanic tuffs, obtaining three filtered samples from each. All initial and filtrated samples were tested for their activity on platelet activating factor (PAF)-induced aggregation. The results showed that the initial samples contain biologically active compounds (PAF inhibitors) and that in their respective last-eluted filtered samples these compounds are purified. These eluted samples, along with their corresponding initial OMWW, were further separated with HPLC and the purified fractions responsible for the aforementioned biological activity, were further studied using chemical determinations and MS analysis. It was confirmed that the PAF inhibitor present in these fractions resembles the one isolated from olive oil. These results offer a new approach on the OMWW handling by offering an alternative use of this waste as starting material for nutritional and/or pharmaceutical purposes in the future.

KEYWORDS: Atherosclerosis; olive mill wastewater; olive oil; PAF; filtration; zeolite; diatomite

INTRODUCTION

Olive mill waste water (OMWW) is a heavily polluting byproduct in all the olive oil producing countries (*1*). In the Mediterranean Basin alone, OMWW accounts for $10-12 \times 10^6$ m^3 of pollution each year (*2*). OMWW is considered one of the "heaviest" biomechanical byproducts mostly due to its organic load, with biochemical oxygen demand (BOD_5) and chemical oxygen demand (COD) that can reach up to 100 and 220 g/L, respectively. Many different methods for the degradation of the wastes have been proposed, the majority of them involving physicochemical and microbial treatment of the wastes (*1*, *3*), while only a few propose extraction of compounds with high biological activity (*4*, *5*). The organic load of OMWW varies greatly according to the harvesting season, the cultivar, the climate and the extraction procedure, so it is difficult to standardize their exact composition. Statistical analyses from a number of studies pointed out that 60% of their dry weight are sugars, followed by phenolic/polyphenolic compounds and oil residues (*1*).

Several studies have investigated the antioxidant properties of olive oil phenolic compounds (*6*−*10*) and their ability to modulate the endothelial function by inhibiting the production of cytokines (*11*, *12*). In another study oral administration of hydrolyzed olive vegetation water (OVW) in mice, a condensed form of OMWW also rich in phenolics, significantly inhibited the production of the inflammatory cytokine TNF-α (*13*). The decrease could not be attributed to hydroxytyrosol, the major phenolic compound present in the OVW, suggesting that another compound, probably a nonphenolic one, decreases TNF-α production both *in vivo* and *in vitro*.

Platelet activating factor (PAF) (*14*), a potent lipid mediator, is synthesized by several different cell types following activation, e.g., platelets, monocytes, macrophages, foam cells and endothelial cells. PAF has been implicated in the propagation of inflammatory responses (*15*), therefore it has been suggested that it is a key molecule in inflammatory diseases, such as atherosclerosis (*16*). A set of *in vitro* studies reported the presence of PAF inhibitors in the polar lipid fractions of olive oil byproducts, including the OMWW (*17*), as well as in the polar lipid extracts of olive oil (OOPL) and pomace (PPL) (orujo). PAF agonists are considered the best PAF inhibitors. These molecules act through PAF receptor, inhibiting PAF biological actions at low concentrations while inducing platelet aggregation at significantly higher concentrations (up to 4 orders of magnitude). The antiatherogenic properties of these agonists/inhibitors were studied when dietary

*Corresponding author. Tel: +30210-7274265. Fax: +30210-7274265. E-mail: demopoulos@chem.uoa.gr.

 Published on Web 10/30/2009

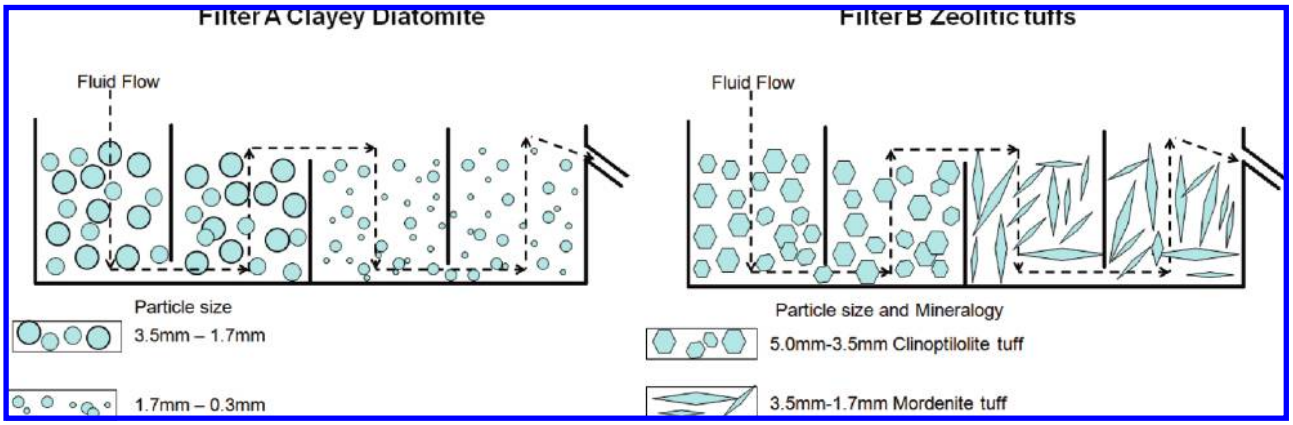

Figure 1. Schematic representation of the filtering device, the fluid flow and the granulometries of the sieved raw materials used.

supplementation of either OOPL or PPL on cholesterol-fed rabbits significantly inhibited the development of atheromatous lesions (*18*, *19*).

The focus of the present study was to investigate and prove the presence of PAF inhibitors in OMWW and the effectiveness of different filtering media for their purification and isolation. The filtering media and the filtration procedure were designed to simulate, in small scale, an efficient and economic waste management system that can be installed in olive oil mills, even at the small "family" mills that represent the majority of the olive mills in Greece.

The raw materials that were used as adsorbents in the study were selected considering their abundance in the olive producing countries, their low cost, minimum ore-processing (*20*), and efficiency for the given application.

MATERIALS AND METHODS

Instrumentation. The photometric measurements were obtained by a Helios β spectrophotometer (Spectronic Unicam, Cambridge, U.K.) equipped with a 7-position automated sample changer. High performance liquid chromatography (HPLC) was performed on a Hewlett-Packard (Agilent Technologies, Waldbronn, Germany) series 1100, equipped with a 100 μL loop Rheodyne (7725 i) injector, a degasser G1322A, a quat-gradient pump G1311A, and an HP UV spectrophotometer G1314A as a detection system. The spectrophotometer was connected to a Hewlett-Packard model HP-3395 integrator-plotter. The analysis of the chromatographs was performed via the Agilent Chemstation software. Phenolics were separated on a Nucleosil-300 7 μm C-18 reverse column (250 × 4.6 mm i.d.) from M-Z Analysentechnik (Woehlerstrasse, Mainz, Germany) with a C-18 ODS (20 × 4.0 mm i.d.) precolumn cartridge. Separation of polar lipids was carried out on a Sphereclone 5 μm NH_2 normal phase column (250 × 4.6 mm i.d.) from Phenomenex (Hurdsfield, Cheshire, U.K.) with an NH_2 silica (20 × 4.0 mm i.d.) precolumn cartridge. All HPLC analyses were performed at room temperature. PAF-induced aggregation was measured in a Chrono-Log (Havertown, PA) aggregometer coupled to a Chrono-Log recorder (Havertown, PA). The electrospray ionization mass spectrometry (ESMS) was performed on an electrospray MS-LCQ-Deca (Thermo Finnigan Ltd., Hertfordshire, U.K.), low-flow mass spectrometer.

Scanning electron microscopy (SEM) was performed on a JEOL JSM-5600 microscope with an OXFORD LINK ISIS energy dispersive X-ray microanalyzer in the National and Kapodistrian University of Athens (NKUA), Athens, Greece. Conditions: acceleration voltage 20 kV, beam current 0.5 nA, lifetime 50 s, beam diameter <2 μm. The X-ray fluorescence was performed on a SIEMENS SRS 3400 at TITAN Cement Company SA, at the Kamari plant, Greece. The X-ray diffraction measurements were carried out at NKUA, Athens, Greece, on a Siemens model 5005 X-ray diffractometer in combination with the DIFFRACplus software package. The diffractometer was operated using Cu Kα radiation at 40 kV and 40 mA and employing the following scanning parameters: 0.020°/s step size. The raw files were evaluated by use of the EVA 10.0 program of the Siemens DIFFRACplus-D5005 software package.

Materials. All reagents and chemicals were of analytical grade supplied from Merck (Darmstadt, Germany). The solvents used for HPLC analyses were purchased from Ruthburn (Walkerburn, Peebleshire, U.K.). All standards, bovine serum albumin (BSA), BN 52021 and DPPH were obtained from Sigma (St. Louis, MO). Olive mill wastewater samples were collected by a 3-phase (OMWW) centrifugal olive mill, in Kyparissia, Peloponnesus, Greece, and the pressing olive mill (OVW) of the Waste Management Laboratory, Department of Environment, University of Aegean, Mytilene, Greece. The term olive mill wastes (OMW) will be used from now on for both types of wastes.

The microporous minerals used for the solid phase extraction (SPE) were (a) clayey diatomite (filter A) originated from Thessaly, Central Greece, and (b) zeolitic volcanic tuffs (filter B) originated from Almeria, Spain, and Samos Island, Greece.

Filter Preparation. The raw materials collected from the field were dried overnight at 75 °C and crushed and sieved in order to achieve the desirable granulometry. The clayey diatomite, being soft, underwent calcination at 800 °C in order to avoid its fluidization during the experiment. The calcination of the sample does not affect its adsorption capacity (*21*). The commercially used adsorbents commonly have grain size ranging from 0.3 to 1.7 mm. In the present study different grain sizes were tested. In order to achieve flow rates up to 1 L/h through the filtering device different combinations of raw materials and/or granulometries were used (Figure **1**). The design of the device maximizes the time that the OMWW stay over the microporous filters. The device is a laboratory scale reproduction of commercially used filtering tanks; specifically it is constructed from INOX steel, its dimensions are 30 × 20 × 20 cm, the width of the separator panels is 0.1 mm and the panels separate the bath into four volumetrically equal chambers as shown in **Figure 1**. The final weight of both the mineral filters was 7.0 kg, specifically in filter A were used 4.0 kg of 3.5−1.7 mm and 3.0 kg of 1.7−0.3 mm. In filter B were used 4.0 kg of Clinoptilolite-type zeolitic tuff and 3.0 kg of Mordenite-type zeolitic tuff.

Extraction of Total Lipids and Phenols. Total lipids (TL) were extracted according to the Bligh−Dyer method (*22*) and were further separated into polar lipids (PL) and neutral lipids using the countercurrent distribution (*23*). Briefly, 10.0 mL of the TL solution was separated using this method and the resulting PL were evaporated under nitrogen current and diluted in 10.0 mL of chloroform/methanol (1:1 v/v) solution. The mineral filters were homogenized, and a small sample was treated as above.

For the extraction of phenols 2.5 L of methanol is added to 1 L of the initial sample of OMW in order to achieve methanol/water 60/40. The mixture is then washed with 1.25 L of *n*-hexane twice (*24*), thus obtaining the phenol-rich extract (PR).

HPLC Separation of OMWW Polar Lipids. Separation of polar lipids was performed on a normal phase NH_2 column with a gradient elution system (*17*). The following solvents and elution profiles were used: solvent A, acetonitrile/methanol (60:40 v/v); solvent B, methanol (100%); solvent C, water (100%); elution profile, 0−35 min, 100% A (isocratic elution); 35−40 min, 40−100% B (linear gradient); 40−45 min, 100% B;

Table 1. Mineralogical Analysis of the Microporous Filters

	semiquantitative analysis[a]		
		zeolitic tuffs	
minerals	clayey diatomite	Almeria	Samos
clinoptilolite	ND	ND	MJ (∼90%)
mordenite	ND	MJ (∼70%)	ND
vermiculite	TR	ND	ND
smectite	MD	MD	TR
opal-A[b]	MJ [∼50%]	ND	ND
opal-CT[c]	ND	MD	TR
illite/muscovite	MD	TR	TR
feldspars	TR	TR	TR
quartz	TR	TR	TR

[a] MJ: major component. MD: medium component. TR: minor to trace component. ND: not detected. [b] Points opal-A being amorphous as detected by SEM and by the hump of the XRD diagram at 20−26°. [c] Points opal-CT being a semicrystalline silica polymorph.

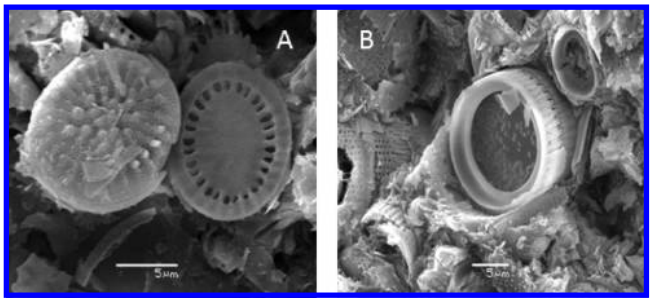

Figure 2. SEM images of the clayey diatomite of Elassona-Sarantaporo. (**A**) Disc-shaped diatom frustules, that represent the opal-A. Their microporous structure is obvious. (**B**) Cylindrical diatom frustules predominate in the clayey diatomite, hosted in a smectite-vermiculite (bentonitic) rich groundmass. The porous structure of the minerals is clearly shown.

45−50 min, 0−100% C (linear gradient); 50−60 min, 100% C. The flow rate for the separation of the lipid classes was 1 mL/min, and the UV detector was operating at 208 nm.

HPLC Separation of OMW Phenols. From the initial 10 mL of PL solution, 7.5 mL was injected into the HPLC through injections of 100 μL each. The distinctive peaks of the chromatograph were collected separately, and in the absence of a peak the samples were collected according to their elution time. Each of the collected HPLC fractions was evaporated using a flash evaporator and dissolved in chloroform/methanol (1:1 v/v) to a final volume of 10.0 mL.

Separation was performed on a Nucleosil-300 C-18 column and a stepped gradient elution system (*24*) with the following solvents and elution profiles: solvent A, water/acetic acid (100:1 v/v); solvent B, methanol/acetic acid (90:1); solvent C, acetonitrile; elution profile, 0−30 min, 90% A/9% B/1% C to 70% A/27% B/3% C (gradient linear); 30−35 min, 70% A/27% B/3% C (isocratic elution); 35−45 min, 60% A/36% B/4% C (gradient linear); 45−60 min, 50% A/45% B/5% C; 60−70 min, 0% A/90% B/10% C; 70−80 min, 0% A/90% B/10% C (isocratic elution). The flow rate for the separation of the lipid classes was 1 mL/min, and the UV detector was operating at 280 nm.

Biological Assay. TL and PL, as well as the purified fractions obtained by the above-mentioned HPLC separations, were tested for their biological activity to induce aggregation or to inhibit PAF-induced aggregation on washed rabbit platelets. PAF and the examined samples were evaporated under nitrogen current and redissolved in 2.5 mg of bovine serum albumin (BSA)/mL of saline. The aggregatory effect of a given sample is expressed by reference to a nine point regression curve as PAF concentration. In order to determine the inhibitory effect of each sample, the platelet aggregation induced by PAF (5×10^{-11} M, final concentration) was measured in the absence (0% inhibition) and in the presence of various volumes of each sample. Consequently, the plot of percent inhibition (ranging from 20 to 80%) versus different sample volumes is linear. From this curve, the concentration of the sample that inhibited 50% PAF-induced aggregation was calculated, and this value was defined as IC_{50}. Desensitization experiments were performed using PAF and the HPLC fractions. The fractions that exhibited aggregatory activity were further studied in the presence of the specific PAF receptor inhibitor BN 52021 (0.1 μM) (*25*). The experiments were repeated thrice with different batches of washed platelets.

Table 2. Chemical Analysis of the Microporous Filters

	% content		
		zeolitic tuffs	
oxides	clayey diatomite	Almeria	Samos
Na_2O	1.01	1.92	0.52
K_2O	2.47	2.15	4.85
CaO	1.30	2.05	2.40
MgO	1.85	1.06	1.65
MnO	ND[a]	0.03	0.06
Fe_2O_3t	4.65	1.44	2.56
TiO_2	0.76	0.11	0.17
Al_2O_3	15.20	11.29	15.28
SiO_2	67.20	67.50	61.33
P_2O_5	ND	0.04	0.05
LOI	5.53	11.39	11.04
SrO	ND	0.13	0.12
total	99.88	99.11	100.03

[a] ND: not detected.

Treatment with PAF-acetylhydrolase. The effect of rabbit plasma PAF-acetylhydrolase (PAF-AH), an enzyme specific to short or intermediate length *sn-2* chains, was examined on the fractions that induced platelet aggregation. Briefly, 50 μL of Tris buffer (50 mM, pH 7.4) and the examined sample in BSA (2.5 mg/mL saline) were added to a prewarmed (37 °C) test tube. The aggregatory activity of this solution is considered the activity at zero time. Afterward rabbit serum PAF-acetylhydrolase was added to the test tube and at different time intervals aliquots were taken to test their ability to induce aggregation on washed rabbit platelets (*25*). The same procedure is followed with PAF at concentrations that induce the same aggregation with the tested samples.

Chemical Determinations. *Phenol Determination*. Samples are evaporated under nitrogen current, and 3.5 mL of water and 0.1 mL of Folin−Ciocalteu reagent are added to them. The samples are shaken, and after 3 min, 0.4 mL of Na_2CO_3 35% (w/v) is added. The sample mixture is left to react for 1 h, and the samples are measured at 725 nm (*26*). The results are expressed by reference to a six point regression curve, as μg of gallic acid equivalents per mL of sample (μg GAE/mL).

o-Diphenol Determination. Samples are evaporated under nitrogen current, and 3.6 mL of ethanol 50% is added. The samples are shaken, 400 μL of Na_2CO_3 5% w/v in aqueous ethanol 50% is added and the samples are left to react for 15 min. The samples are measured at 370 nm (*27*). The results are expressed by reference to a six point regression curve, as μg of caffeic acid equivalents per mL of the sample (μg CAE/mL).

Determination of the Different Phenolic Classes. Samples are evaporated under nitrogen stream, and 400 μL of ethanol 95% acidified with HCl 0.1% is added. The samples are shaken, and 3.6 mL of HCl 2% (v/v) is added. The samples are then measured at 320 nm for the determination of hydroxycinnamic acid using caffeic acid as standard and at 360 nm for the determination of flavonoids using quercetin as standard. The results are expressed as μg of caffeic acid or quercetin equivalents per mL of the sample for the quantification of hydroxycinnamic acid and flavonoids respectively (*28*).

Sugar Determination. Sugar determination was carried out according to the method of Galanos and Kapoulas (*29*). The results are expressed by reference to a six point regression curve as μg of glucose per mL of the sample (μg Glu/mL).

Determination of the Antioxidant Activity of the Samples with the DPPH Assay. The assay is based on the scavenging of 2,2-diphenyl-1-picrylhydrazyl radical (DPPH$^{\bullet}$) (*30*). Various concentrations were made for each tested sample in ethanol. DPPH$^{\bullet}$ was then added in these ethanol solutions, and the whole mixture was incubated at 37 °C for

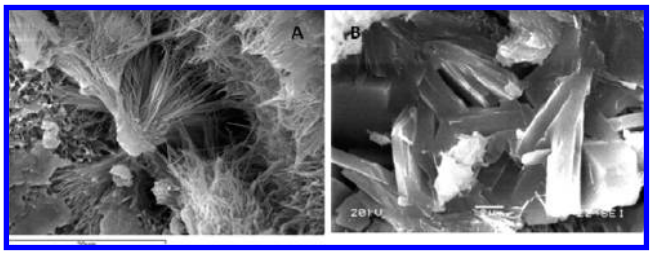

Figure 3. SEM images of the zeolitized tuffs studied. (**A**) Fibrous aggregates of mordenite crystals (Almeria). (**B**) Euhedral clinoptilolite crystals forming tabular aggregates (Samos).

30 min. Scavenging of DPPH• was determined by measuring the absorbance of samples at 516 nm. DPPH-EC_{50} represents the sample concentration that induced 50% scavenging of DPPH• and is expressed as μL of the extract. The concentration of DPPH is calculated prior to the sample measurements.

Mass Spectrometry. Data were acquired over the appropriate m/z range and spectra processed using the XCalibur software supplied with the mass spectrometer; MS-LCQ-Deca (Thermo Finnigan), low flow mass spectrometer. Samples were dissolved in a small volume of HPLC grade methanol/water (70:30, v/v) 0.01 M in ammonium acetate.

Electrospray samples are typically introduced into the mass analyzer at a rate of 3 μL/min. Nitrogen of purity 99.99% is used as nebulizing gas and as bath gas with flow rate 3 μL/min. The spectrum analysis was conducted in the ion space of 50−1500 m/z, and the conditions for the highest intensity of the summits with the lowest rupture were those that are shown below: spray voltage = 5 kV, capillary voltage = 7 V, capillary temperature = 275 °C, lens-entrance voltage = −54 V, lens voltage = −22 V.

Mass Spectrometry Data Analysis. The MS data were processed by a software application, which was developed in order to automatically handle the MS interpretation, since manual interpretation of MS and processing of the results often requires a great amount of time. It must be noted that, to the best of our knowledge, this is a new approach of software that attempts to extract information from MS based on unknown samples. The software will be further developed in order to simultaneously quantify the studied compounds, and the entire application will be published in detail elsewhere. Briefly, the application was developed for execution under Microsoft Windows XP Operating System, and more specifically, the Graphical User Interface (GUI) was implemented in Visual Basic.NET 2008 while the time-consuming functions were implemented in GNU C, for superior performance.

The MS data are extracted in a tabulated ASCII format file from the mass spectrometer software (XCalibur), which is used as an input file for the developed application. Initially the data are filtered, based on the desired range for the m/z and the intensity values, given by the user. The filter data are then sought exhaustively for values that comply with the restrictions and conditions of each studied compound in the MS. Such restrictions can be the difference in the m/z values at positive- and negative-ion electrospray ionization mass spectrometry (ESI MS+/MS−), on the desired range for the m/z and the intensity values, that could be candidates for the possible molecular weights (M) of the studied compound. Using these m/z values for the M, one can search for the existence of expected fragments [M − X] that are specific for the various compound classes or even the existence in ESI MS+/MS− of fragments that added can provide the fragment of the molecular weight. This procedure reveals m/z values that could be candidates for the calculation of possible M and X group(s) of the molecule. Finally, one can detect the m/z values that comply to all (or to the desired combinations) of the aforementioned restrictions. So, one could have the molecular weight along with some (or all) constituents of the studied molecule, and—arranging the puzzle—could elucidate the structure of the unknown molecule. In the case of missing some pieces of the puzzle, with a feedback procedure one may find out the group(s) that matches to the missing constituents of the studied molecule. All the above-mentioned user choices are given via the GUI, and the results are also presented on screen and additionally extracted to an output file.

Table 3. Nomenclature and Description of the Samples[a]

sample name	description
	Kyparissia OMWW/Filter A (Diatomite)
K_A P	1 L of initial OMWW extracted for the recovery of phenols
K_A L	1 L of initial OMWW extracted for the recovery of total lipids
K_A 1	1st liter of filtered OMWW extracted for the recovery of total lipids
K_A 2	2nd liter of filtered OMWW extracted for the recovery of total lipids
K_A 3	3rd liter of filtered OMWW extracted for the recovery of total lipids
	Kyparissia OMWW/Filter B (Zeolites)
K_B L	1 L of initial OMWW extracted for the recovery of total lipids
K_B 1	1st liter of filtered OMWW extracted for the recovery of total lipids
K_B 2	2nd liter of filtered OMWW extracted for the recovery of total lipids
K_B 3	3rd liter of filtered OMWW extracted for the recovery of total lipids
	Mytilene OVW/Filter A (Diatomite)
M_A P	1 L of initial OVW extracted for the recovery of phenols
M_A L	1 L of initial OVW extracted for the recovery of total lipids
M_A 1	1st liter of filtered OVW extracted for the recovery of total lipids
M_A 2	2nd liter of filtered OVW extracted for the recovery of total lipids
M_A 3	3rd liter of filtered OVW extracted for the recovery of total lipids
	Mytilene OVW/Filter B (Zeolites)
M_B L	1 L of initial OVW extracted for the recovery of total lipids
M_B 1	1st liter of filtered OVW extracted for the recovery of total lipids
M_B 2	2nd liter of filtered OVW extracted for the recovery of total lipids
M_B 3	3rd liter of filtered OVW extracted for the recovery of total lipids

[a] The letters "M" or "K" stand for "Mytilene" or "Kyparissia", respectively, whereas the letters "A" or "B" indicate the filtering media. The third letter, either "L" or "P", stands for the extraction method used, lipids or phenols, and the numbers correspond to the first, second and third liters that went through the filtering media.

Table 4. Results of the Biological Assay of the Sample TL

sample name	inhibition (IC_{50})[a]	aggregation
K_A P	0.28 ± 0.06	ND[b]
K_A L	0.16 ± 0.04	ND
K_A 3	0.3 ± 0.07	1.1 ± 0.2[c]
K_B L	0.2 ± 0.09	0.9 ± 0.08[c]
K_B 3	d	0.25 ± 0.09[c]
M_A P	0.18 ± 0.08	ND
M_A L	0.16 ± 0.04	ND
M_A 3	d	ND
M_B L	0.24 ± 0.07	ND
M_B 3	4.3 ± 0.8	ND

[a] The results of IC_{50} are expressed in μL of the initial extract. [b] ND: not detected. [c] Slow non-PAF-like platelet aggregation. [d] Very potent inhibition of PAF-induced aggregation, with IC_{50} lower than 0.1 μL.

RESULTS AND DISCUSSION

Raw Materials. The microporous raw materials used as filters in the present study are abundant in the olive producing countries and also of low cost. Both the microporous raw materials used have good adsorbing capacity for the organic load of OMW as shown in previous studies (*31*, *32*). The raw materials were characterized mineralogically, chemically and texturally using XRD, XRF and SEM respectively.

The clayey diatomite (filter A) mainly consists of small, well-preserved diatom frustules (biogenic opal-A) and clayey mineral microparticles (Table **1** and Figure **2**). Furthermore, the raw material is characterized by the predominance of silica and alumina (Table **2**). The zeolite rich volcanic tuffs (filter B) mainly consist of the zeolite minerals mordenite (Almeria) or clinoptilolite (Samos). The Almeria sample also contains the silica polymorph opal-CT, which forms small lepispheres, and the clay

Table 5. Inhibitory Effect against PAF Induced Platelet Aggregation Performed on the HPLC Fractions from OMW

	inhibition (RT)[a]								
HPLC fr	K_A P	K_A L	K_A 3	K_B L	K_B 3	M_A L	M_A 3	M_B L	M_B 3
1	158 ± 25 (0−9.8)	− (0−10)	− (0−10)	16 ± 4 (0−5.8)	8 ± 1 (0−10)	− (0−9,8)	− (0−10)	− (0−10)	56 ± 7 (0−10)
2	254 ± 29 (9.8− 14)	192 ± 22 (10−15)	273 ± 22 (10−15)	21 ± 7 (5.8−8)	− (10−20)	278 ± 27 (9.8− 20)	286 ± 27 (10−14)	212 ± 12 (10−22)	750 ± 29 (10−19)
3	161 ± 26 (14−22)	360 ± 29 (15−22)	518 ± 31 (15−22)	− (8−15)	− (20−30)	236 ± 30 (20−30)	151 ± 11 (14−25)	208 ± 32 (22−31)	213 ± 29 (19−25)
4	236 ± 31 (22−27)	192 ± 18 (22−30)	206 ± 15 (22−30)	20 ± 8 (15−25)	63 ± 15 (30−35)	158 ± 11 (30−38)	130 ± 14 (25−31)	230 ± 15 (31−38)	− (25−35)
5	313 ± 30 (27−38)	210 ± 20 (30−38)	56 ± 11 (30−38)	5 ± 2 (25−35)	− (35−45)	360 ± 15 (38−45)	− (31−38)	180 ± 11 (38−45)	375 ± 31 (35−39)
6	276 ± 27 (38−44)	640 ± 35 (38−50)	210 ± 41 (38−50)	3 ± 1 (35−38)	80 ± 25 (45−50)	366 ± 19 (45−50)	640 ± 24 (38−44)	133 ± 12 (45−50)	124 ± 12 (39−44)
7	214 ± 20 (44−50)	− (50−60)	27 ± 9 (50−60)	13 ± 5 (38−45)	115 ± 14 (50−60)	100 ± 13 (50−60)	300 ± 27 (44−50)	180 ± 29 (50−60)	− (44−50)
8	15 ± 3 (50−60)			43 ± 22 (45−50)			327 ± 22 (50−60)		127 ± 12 (50−60)
9				115 ± 12 (50−60)					

[a] Inhibition: IC_{50} is expressed in μL of the collected sample; its retention time (RT) in minutes is also stated. [b] The inhibitions marked with "−" were very potent, and the calculation of IC_{50} was very difficult.

Table 6. Aggregatory Effect of the HPLC Fractions from OMW

	aggregation[a]								
HPLC fr	K_A P	K_A L	K_A 3	K_B L	K_B 3	M_A L	M_A 3	M_B L	M_B 3
1	ND (0−9.8)	ND (0−10)	ND (0−10)	ND (0−5.8)	ND (0−10)	ND (0−9.8)	ND (0−10)	ND (0−10)	ND (0−10)
2	0.3/c (9.8− 14)	1/c (10−15)	1/c (10−15)	ND (5.8−8)	0.5[b]/ 1.23 ± 0.39 (10−20)	ND (9.8− 20)	ND (10−14)	ND (10−22)	ND (10−19)
3	0.3/c (14−22)	ND (15−22)	ND (15−22)	0.5[b]/ 1.82 ± 0.26 (8−15)	0.4[b]/ 1.82 ± 0.27 (20−30)	2/c (20−30)	0.3/c (14−25)	1[b]/ 1.01 ± 0.23 (22−31)	ND (19−25)
4	ND (22−27)	1[b]/ 0.56 ± 0.08 (22−30)	1[b]/ 0.94 ± 0.09 (22−30)	ND (15−25)	ND (30−35)	1/c (30−38)	0.3/c (25−31)	2/c (31−38)	0.75[b]/ 2.19 ± 0.27 (25−35)
5	1[b]/ 0.33 ± 0.01 (27−38)	1[b]/ 1.22 ± 0.07 (30−38)	1[b]/ 1.93 ± 0.13 (30−38)	0.7[b]/ 0.93 ± 0.15 (25−35)	0.8[b]/ 2.39 ± 0.33 (35−45)	1/c (38−45)	0.2[b]/ 2.96 ± 0.33 (31−38)	1/c (38−45)	0.75/c (35−39)
6	1/c (38−44)	1[b]/ 0.58 ± 0.11 (38−50)	1/c (38−50)	1.2[b]/ 1.93 ± 0.23 (35−38)	0.8/c (45−50)	ND (45−50)	0.1[b]/ 2.99 ± 0.39 (38−44)	ND (45−50)	0.75[b]/ 0.92 ± 0.28 (39−44)
7	1/c (44−50)	0.3[b]/ 1.93 ± 0.25 (50−60)	0.1[b]/ 2.17 ± 0.31 (50−60)	0.4/c (38−45)	0.1/c (50−60)	0.3/c (50−60)	1/c (44−50)	1/c (50−60)	2[b]/ 2.52 ± 0.31 (44−50)
8	0.8[b]/ 0.5 ± 0.08 (50−60)			0.8/c (45−50)			0.3/c (50−60)		1/c (50−60)
9				0.5/c (50−60)					

[a] Aggregation: Results are expressed as mL of the collected fraction, unless otherwise stated, and (/) the equivalent concentration of PAF (expressed as $\times 10^{-11}$ M) that exerts in platelets the same biological activity as the amount of fraction; its retention time (RT) in minutes is also stated. ND: not detected. [b] These samples cause PAF-like aggregation. [c] Slow non-PAF-like platelet aggregation.

Table 7. Results of the Chemical Determinations of the Samples[a]

sample	biol activ	sugars (μg Glu/mL)	Folin−Ciocalteau (μg GAE/mL)	*o*-diphenols (μg CAE/mL)	hydroxycinnamic (μg CAE/mL)	flavonoids (μg QAE/mL)
K_A P fr 1		797.3 ± 23.1	56.3 ± 6.2	10.6	6.8	25.9
K_A P fr 3		55.1 ± 12.3	10.7 ± 3.9	7.3	6.5	2.7
K_A P fr 5	+	45.8 ± 13.1	5.7 ± 3.3	4.5	3.7	0.0
K_A P fr 6	+	52.3 ± 22.2	5.3 ± 12.6	3.8	3.8	0.0
K_A P fr 7	+	49.15 ± 23.5	21.9 ± 7.4	12.5	13.4	2.0
K_A L fr 1		94.7 ± 32.1	43.8 ± 6.2	9.6	30.5	25.7
K_A L fr 4	+	24.3 ± 3.2	3.8 ± 1.1	3.4	2.6	0.0
K_A L fr 5	+	25.5 ± 3.7	3.4 ± 2.3	2.8	3.3	0.0
K_A L fr 7	+	29.5 ± 4.5	11.4 ± 4.2	4.3	3.6	8.9
K_A 3 fr 1		95.9 ± 11.5	21.0 ± 3.3	10.9	14.9	17.3
K_A 3 fr 5	+	19.1 ± 2.6	3.4 ± 2.1	3.2	0.9	0.4
K_A 3 fr 6	+	23.2 ± 3.6	7.8 ± 1.1	3.0	4.0	0.0
M_A L fr 1		132.9 ± 19.4	88.8 ± 8.5	24.3	25.5	27.1
M_A L fr 3	+	19.5 ± 3.4	4.0 ± 3.6	3.4	3.2	0.0
M_A 3 fr 1		131.7 ± 19.2	82.9 ± 3.6	15.2	15.4	12.4
M_A 3 fr 5	+	15.4 ± 1.1	2.8 ± 1.2	2.7	3.3	0.0
M_A 3 fr 6	+	16.2 ± 3.3	2.4 ± 1.1	2.8	3.6	0.0
M_B L fr 1		169.5 ± 13.5	112.4 ± 12.6	29.0	20.6	17.4
M_B L fr 3	+	25.1 ± 3.8	4.9 ± 1.6	4.0	3.9	0.0
M_B L fr 4		22.9 ± 4.1	2.8 ± 1.1	2.7	2.7	0.0
M_B L fr 6	+	22.1 ± 4.3	2.2 ± 1.0	2.0	2.9	0.0
M_B L fr 7		34.3 ± 3.1	11.4 ± 3.9	5.9	6.8	2.0
M_B 3 fr 1	+	136.2 ± 15.5	77.4 ± 14.6	13.3	33.3	40.9
M_B 3 fr 2		19.2 ± 3.5	3.0 ± 1.6	4.8	5.7	3.6
M_B 3 fr 4	+	27.7 ± 7.6	3.4 ± 1.6	3.3	4.5	0.0
M_B 3 fr 8	+	26.9 ± 6.1	9.0 ± 3.1	6.0	6.7	1.6
M_A P		21729.6 ± 356.6	5459.2 ± 45.6	3180.0	1168.9	621.0
M_A L		45.1 ± 6.2	598.4 ± 22.5	ø	ø	ø
M_A 1		48.8 ± 3.2	481.3 ± 12.6	ø	ø	ø
M_A 2		42.4 ± 3.1	366.0 ± 10.6	ø	ø	ø
M_A 3		32.4 ± 5.3	386.9 ± 11.7	ø	ø	ø
M_B L		212.8 ± 11.1	670.4 ± 23.3	ø	ø	ø
M_B 1		49.6 ± 4.1	359.7 ± 13.3	ø	ø	ø
M_B 2		51.5 ± 2.2	343.7 ± 8.4	ø	ø	ø
M_B 3		45.5 ± 2.2	319.7 ± 8.7	ø	ø	ø
K_A P		12840.7 ± 190.1	2167.5 ± 56.8	3150.0	588.8	154.9
K_A L		27.4 ± 5.3	278.4 ± 12.5	ø	ø	ø
K_A 1		33.3 ± 3.5	231.7 ± 10.1	ø	ø	ø
K_A 2		23.7 ± 3.3	180.5 ± 9.8	ø	ø	ø
K_A 3		25.5 ± 6	142.8 ± 7.8	ø	ø	ø
K_B 3 fr 1		214.6 ± 1.5	32.0 ± 3.2	ø	ø	ø
K_B 3 fr 2	+	25.5 ± 3.4	4.0 ± 1.6	ø	ø	ø
K_B 3 fr 3		17.4 ± 2.4	2.0 ± 0.5	ø	ø	ø
K_B 3 fr 4		6.0 ± 1.4	5.3 ± 1.3	ø	ø	ø
K_B 3 fr 5	+	36.9 ± 4.6	1.0 ± 0.3	ø	ø	ø
K_B 3 fr 6	+	12.4 ± 3.5	1.4 ± 0.6	ø	ø	ø
K_B 3 fr 7		13.3 ± 3.7	3.2 ± 1.0	ø	ø	ø
K_B L fr 1		264.6 ± 12.2	38.4 ± 3.7	ø	ø	ø
K_B L fr 2		15.5 ± 5.3	3.6 ± 0.1	ø	ø	ø
K_B L fr 3	+	22.4 ± 9.4	6.3 ± 1.7	ø	ø	ø
K_B L fr 4		11.0 ± 3.5	3.6 ± 1.3	ø	ø	ø
K_B L fr 5	+	15.1 ± 3.7	2.6 ± 1.6	ø	ø	ø
K_B L fr 6	+	15.5 ± 3.8	1.0 ± 0.4	ø	ø	ø
K_B L fr 7		18.7 ± 4.2	3.0 ± 0.4	ø	ø	ø
K_B L fr 8		9.2 ± 2.1	2.3 ± 0.3	ø	ø	ø
K_B L fr 9		36.5 ± 3.1	9.4 ± 1.7	ø	ø	ø

[a] Results are expressed as μg of the standard (GLU, glucose; GAE, gallic acid) used for the quantification of results as mentioned in Materials and Methods, per mL of the samples as defined in the text. Results are mean ± standard deviation from triplicate analyses. The samples marked with (ø) were not tested.

mineral smectite. The results are presented in **Table 1**. The chemical analysis of the minerals consisting filter B characterizes them as aluminosilicate minerals (**Table 2**). SEM analysis revealed that mordenite has its characteristic fibrous structure whereas clinoptilolite has tabular form (Figure **3**).

Filtering of the OMW. Both OMWW from the two different olive oil mills were divided in half, and the first half passed through filter A and the second half through filter B. Fifteen liters of OMW was poured through the given filtering media, and the first 3 L that went through the exit of the filtering bath was collected separately to obtain 3 samples. The same procedure was applied for the 4 different filtering media/OMW.

The filtered OMW and 1 L of the initial OMW were extracted to recover its TL, whereas another 1 L of the initial OMW that

went though filter A was extracted to recover the phenols. The nomenclature and description of the samples are shown in Table **3**.

Table 8. The Antioxidant Activity of Selected HPLC Fractions[a]

sample	DPPH-EC_{50} (μL)	sample	DPPH-EC_{50} (μL)
K_A P fr 1	115.8 ± 11.2	M_A 3 fr 5	782.8 ± 12.6
K_A P fr 3	423.0 ± 19.3	M_A 3 fr 6	727.6 ± 60.6
K_A P fr 5	≫800.0	M_B L fr 1	32.5 ± 3.5
K_A P fr 6	≫800.0	M_B L fr 3	700.7 ± 25.7
K_A P fr 7	289.8 ± 17.3	M_B L fr 4	≫1500.0
K_A L fr 1	187.0 ± 11.5	M_B L fr 6	566.9 ± 22.2
K_A L fr 5	≫1200.0	M_B L fr 7	771.8 ± 11.1
K_A L fr 7	366.6 ± 13.5	M_B 3 fr 1	68.2 ± 2.9
K_A 3 fr 1	484.4 ± 16.7	M_B 3 fr 2	≫300.0
K_A 3 fr 5	≫1200.0	M_B 3 fr 4	≫900.0
K_A 3 fr 7	≫600.0	M_B 3 fr 8	338.5 ± 19.2
M_A L fr 1	60.9 ± 4.6	K_A P	2.45 ± 0.03
M_A L fr 3	≫900.0	M_A P	0.66 ± 0.03
M_A 3 fr 1	77.2 ± 5.2		

[a] Results are expressed as μL of samples, as defined in the text, that inhibited DPPH radical by 50%. Results are mean ± standard deviation from triplicate analyses.

Biological Assay. The TL samples produced as described above were tested regarding their biological activity on washed rabbit platelets. The results (Table **4**) indicated that all the initial samples exhibited biological activity by inhibiting PAF induced platelet aggregation. The collected samples from each filtration also inhibited PAF-induced aggregation at different potencies than that of their respective initial (unfiltered) sample. The comparison between the initial samples and their third extracted liter in all the samples (with the exception of M_B 2) points out that a better separation/purification of the biologically active compounds present in the initial samples was achieved through the filtration using the aforementioned microporous materials.

Previous studies have reported that the PL fraction contains the biologically active lipids that inhibit PAF-induced aggregation (*17*, *25*). Therefore, PL fractions exerting notable biological activity, as well as the initial samples, were then separated using HPLC with a NH_2 silica column. The collected HPLC fractions were tested for their biological activity. The results (Tables **5** and **6**) show that the majority of the fractions inhibited PAF-induced aggregation. The rest of the fractions exhibited a dual activity of inhibiting PAF-induced aggregation in low concentrations, but inducing platelet aggregation in high concentrations

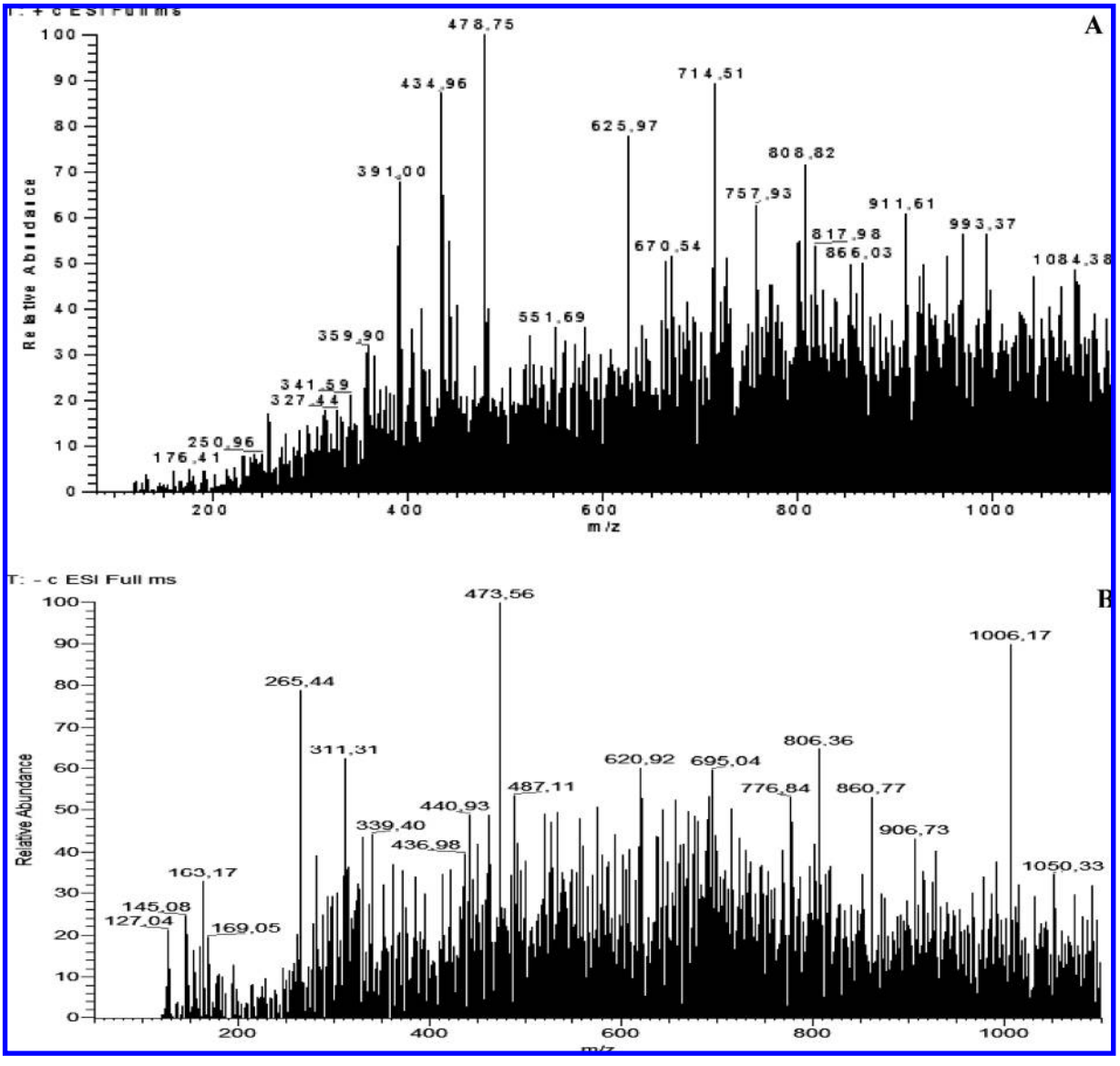

Figure 4. Positive (**A**) and negative (**B**) ion ES/MS of fraction 5 of sample K_B 3.

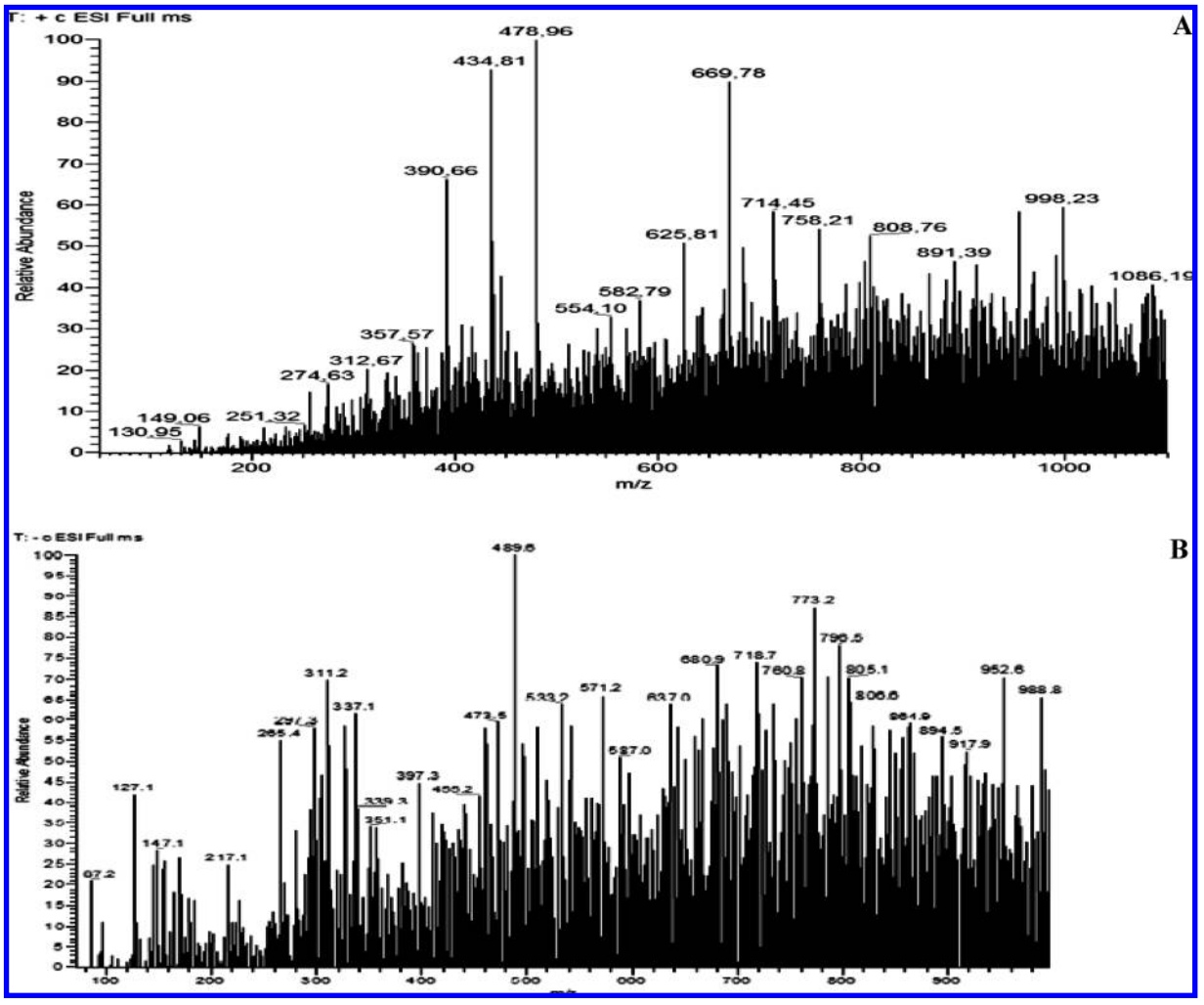

Figure 5. Positive (**A**) and negative (**B**) ion ES/MS of fraction 6 of sample K_B L.

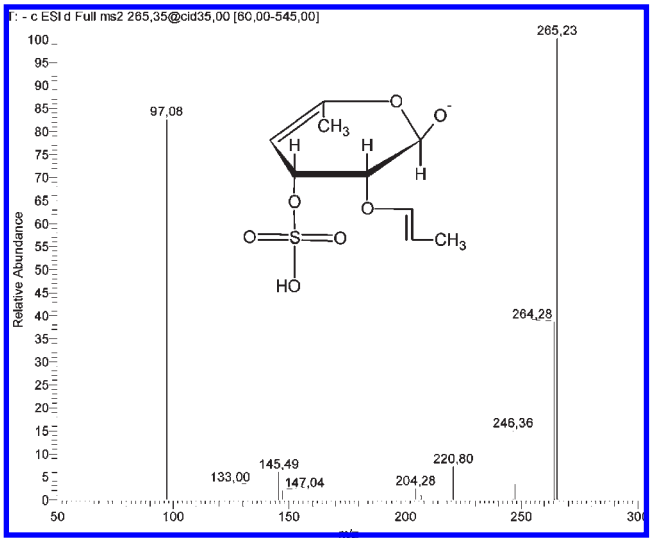

Figure 6. Tandem mass spectrum of ion $[265]^-$.

therefore acting as PAF-agonists. However, the majority of highly potent PAF-agonists are eluted after 35 min as previously reported (*17*, *25*). BN 52021 inhibited the PAF-like aggregation induced by these fractions. Moreover, the fractions desensitized the PAF-induced platelet aggregation, whereas incubation of the aforementioned fractions with PAF-AH resulted in their time-dependent inactivation. This inactivation was similar to that observed when incubating PAF with PAF-AH. All these suggest that the biologically active lipids present in the HPLC fractions act through the PAF signaling pathway and that an acetyl group is present at the *sn-2* position of a glycerol backbone. The activity of the PAF agonists increases in the HPLC fractions of the samples filtered through the microporous mineral filters (**Tables 5** and **6**). This increment can be attributed to the removal of the coeluted PAF antagonists, which can also inhibit the activity of the agonists, masking their effect on platelets.

Chemical Determinations. The initial and filtered OMW as well as the fractions collected from HPLC were further characterized by a series of chemical determinations and the DPPH assay. Regarding the HPLC fractions, results (Tables **7** and **8**) revealed that the majority of the phenolic compounds eluted with short retention times, whereas the majority of the compounds acting as PAF agonists eluted with longer retention times (**Tables 5**−**8**).

From the phenolic content of the samples in conjunction with the sugar determination and the different phenolic subclass determinations (**Table 7**) it became apparent that fraction 5 of sample K_B 3 and fraction 6 of sample K_B L had the best enrichment in sugars against their phenolic content, pointing out that the PAF agonist present in these fractions is a glycolipid (contains sugar moieties) without phenolic moieties. The retention times (RT) (**Tables 5** and **6**) of these two collected samples further confirm this, since they are eluted in the area of the

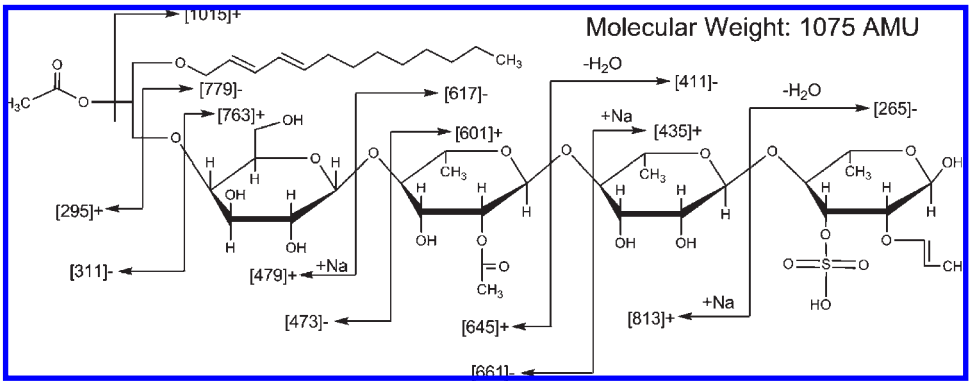

Figure 7. The proposed chemical structure of the biologically active lipid isolated in HPLC fraction 5 of sample K_B 3.

chromatogram where PAF agonists mainly containing sugar and no phenolic moieties are eluted (*17*, *25*).

Additionally the antioxidant activity of some selected HPLC fractions and that of the initial samples K_A P and M_A P measured by the DPPH assay correlate with their phenolic content but not with the anti-PAF activity (**Tables 5**−**8**).

MS Spectra. In order to verify the chemical structure of the biologically active lipid, fraction 5 of sample K_B 3 and fraction 6 of sample K_B L were further analyzed by mass spectrometry. The comparison of the mass spectra from the two samples indicates the enrichment or purification of the biologically active fraction of sample K_B 3 as pointed out from the increased abundance of specific fragments as opposed to the initial sample (Figures **4** and **5**). This increment correlates with the higher biological activity of the fraction (**Table 5**) suggesting that these fragments correspond to the biologically active lipid. Use of the software specifically developed for this analysis further contributed in the interpretation of the spectral data. Specifically by applying desired restrictions on the differences in the *m*/*z* values and seeking for the existence of (expected) fragments, the software automatically located particular *m*/*z* values in the spectrum. These spectral data in conjunction with the aforementioned data obtained from the biological assay support the proposed chemical structure for the molecule as presented in Figure **7**. The molecule in question is a glycerol glycolipid with molecular weight 1075 AMU, evident by $[1074]^-$ (24), $[1076]^+$ (31) and the sodiated $[1098]^+$ (25). The most abundant negative $[473]^-$ (100) and positive $[479]^+$ (100) fragments represent the glycerol backbone substituted at the *sn-3* position by a glucose and its sodiated analogue respectively. The presence of acetic acid at the *sn-2* position pointed from the biological assay is further certified from fragment $[1015]^+$ (30) and the tandem mass spectra of $[473]^-$, which also fragments to $[311]^-$ (61) (data not shown). The loss of a H_2O from the terminal sugar moiety gives rise to $[265]^-$ (85) and the sodiated $[813]^+$ (39). In Figure **6** is presented the tandem mass spectrum of fragment $[265]^-$ with the characteristic abundant fragment of HSO_4^- at m/z = $[97]^-$. The second most abundant positive fragment $[435]^+$ (90), along with $[411]^-$ (35) after the loss of H_2O, corresponds to the loss of the two terminal sugar molecules, whereas the remaining molecule generates the fragments $[661]^-$ (50) and $[645]^+$ (35). Finally the loss of all four sugar moieties generates the fragments $[295]^+$ (17) and $[311]^-$ (61) while the sugar fragment generates $[779]^-$ (44) and $[763]^+$ (34). The fragmentation pattern of $[311]^-$, in particular the absence of a fragment, indicates a glyceryl−ether bond with an unsaturated 13 carbon chain at the *sn-1* position as shown in the proposed molecular structure. The molecular structure of this agonist is similar to that of agonists/inhibitors reported in other studies (*17*, *25*, *33*).

Phenolic Content. In order to assess differences between the two different filtering media (A and B) regarding the adsorption of phenolic compounds, chemical determinations and RP-HPLC analysis were performed on the samples (**Table 7**, Figure **8**). The comparison of some representative samples (**Figure 8**) indicates the adsorption of phenols from the filtering media. The comparison of the initial M_A L with the successive filtered ones through the clayey diatomite extracts and the extract from the filter indicates that the phenolic compounds are adsorbed by the clayey diatomite (Filter A). Some of these adsorbed phenolic compounds are pointed out in the chromatograms with arrows (**Figure 8**). Indicative of the adsorption from M_A 1 to M_A 3 is the reduction of the relative intensity of the peak that elutes at 20 min. The comparison of the filter's extract with the extract of the initial sample further confirms the selective adsorption of several phenolic compounds on the filter A, including the aforementioned peak at 20 min.

The better adsorption efficiency of the clayey diatomite, compared to that of the zeolitic tuffs used, can be attributed to the higher percentage of the smectite-vermiculite minerals it contains. These bentonitic minerals are commonly activated by acidic solutions. The high acidity of the OVW samples promotes H^+ cations to substitute Mg^{2+}, Fe^{3+}, Ca^{2+} and Al^{3+} from the crystal structure of smectite, through cation exchange mechanisms increasing its porosity and subsequently the adsorption efficiency of the filtering media (*34*). The porosity increment can possibly be further amplified through the chelation of the cations released from the smectitic crystal, by the flavonoids present in the wastes (*35*).

OMW handling is a major environmental issue in all the olive producing countries. The phenomenon is climaxed in the Mediterranean Basin in which the majority of the Mediterranean countries are the main olive oil producers worldwide. The limited water recycling/renewal causes oxygen deprivation due to the high BOD_5 and COD of OMW. Furthermore the high concentrations of phenolic compounds in conjunction with the high acidity of OMW create a biotoxic environment at the end points in the sea, disrupting the ecology. Using OMW for other purposes can render the waste useful and may even solve the environmental issues that result from its disposal.

The present study demonstrates that the used microporous materials can separate the OMW samples in order to obtain samples enriched in biologically active compounds that are mainly PAF inhibitors and the phenolic compounds adsorbed on the filtering media that can be re-extracted. Finally the used microporous material can find applications in the construction sector, producing lightweight aggregates or insulation bricks.

Although further studies need to be made in order to maximize efficacy of the proposed filtering method, the results are very

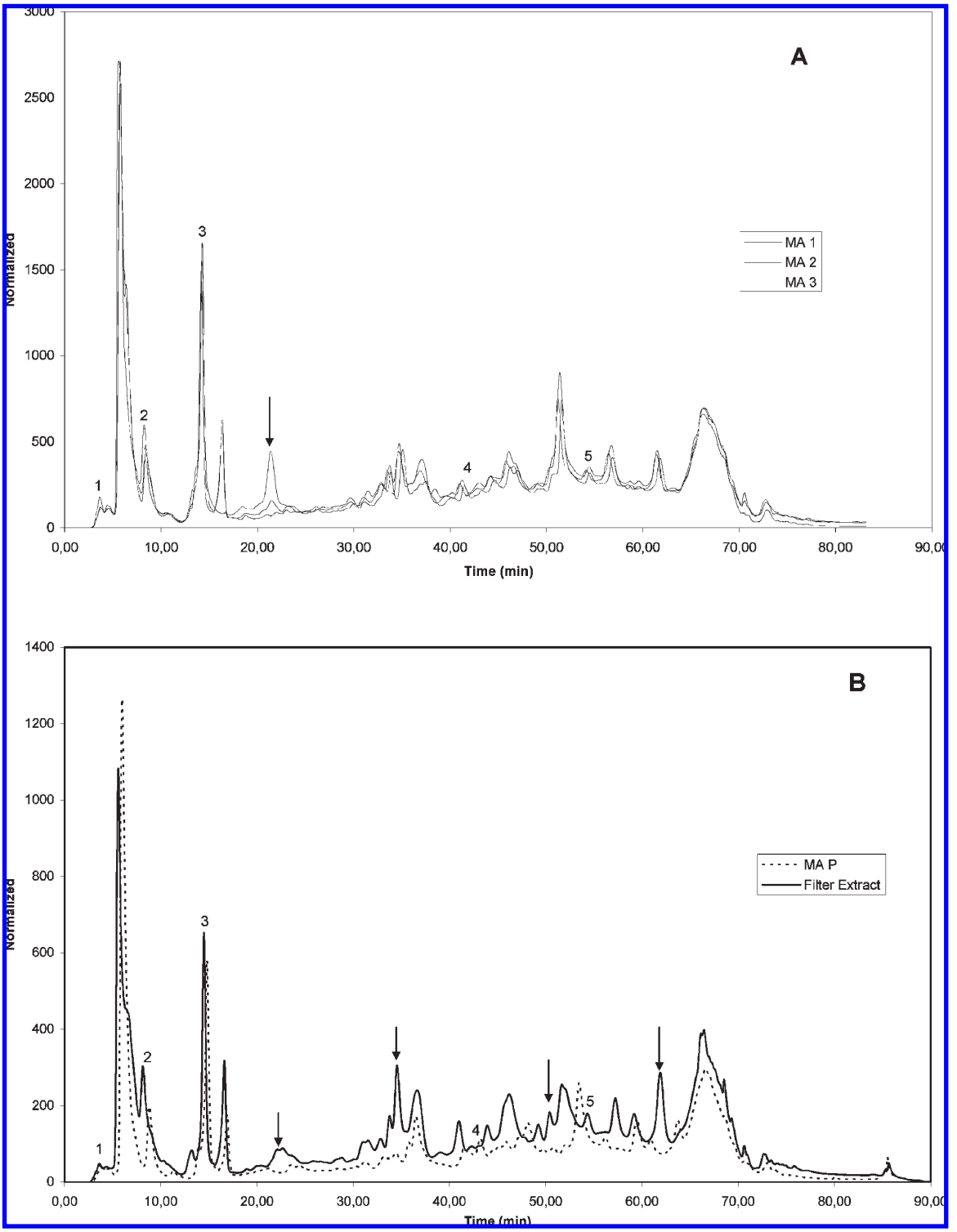

Figure 8. Representative RP-HPLC chromatograms of the samples M_A 1, M_A 2, M_A 3 (**A**) and M_A P, filter A extract (**B**), at 280 nm: 1, gallic acid; 2, tyrosol; 3, caffeic acid; 4, rutin; 5, quercetin. The arrows point out the selective absorption of these phenolic compounds from filter A.

promising, since in this way the filters can be further used after the OMW filtration Moreover, the enriched samples in PAF inhibitors can possibly be used in the future as starting materials to either obtain health beneficiary dietary supplements or isolate these active compounds for pharmaceutical purposes.

ACKNOWLEDGMENT

We thank Professor M. G. Stamatakis, Department of Geology, NKUA, Greece, and D. Fragoulis, TITAN Cement Company, Kamari, Greece, for helping in the fieldwork and XRF analysis respectively.

LITERATURE CITED

(1) Niaounakis, M.; Halvadakis, C. P., *Olive Processing Waste Management—Literature Review and Patent Survey*, 2nd ed.; Diaz, L. F., Ed.; Elsevier: Oxford, U.K., 2006; Vol. 5, pp 1−498.

(2) Cabrera, F.; Lopez, R.; MartinezBordiu, A.; deLome, E. D.; Murillo, J. M. Land treatment of olive oil mill wastewater. *Int. Biodeterior. Biodegrad.* **1996**, *38*, 215–225.

(3) McNamara, C. J.; Anastasiou, C. C.; O'Flaherty, V.; Mitchell, R. Bioremediation of olive mill wastewater. *Int. Biodeterior. Biodegrad.* **2008**, *61*, 127–134.
(4) Capasso, R.; Evidente, A.; Avolio, S.; Solla, F. A highly convenient synthesis of hydroxytyrosol and its recovery from agricultural waste waters. *J. Agric. Food Chem.* **1999**, *47*, 1745–1748.
(5) Agalias, A.; Magiatis, P.; Skaltsounis, A. L.; Mikros, E.; Tsarbopoulos, A.; Gikas, E.; Spanos, I.; Manios, T. A new process for the management of olive oil mill waste water and recovery of natural antioxidants. *J. Agric. Food Chem.* **2007**, *55*, 2671–2676.
(6) Schaffer, S.; Podstawa, M.; Visioli, F.; Bogani, P.; Müller, W. E.; Eckert, G. P. , Hydroxytyrosol-rich olive mill wastewater extract protects brain cells in vitro and ex vivo. *J. Agric. Food Chem.* **2007**, *55*, 5043–5049.
(7) Visioli, F.; Poli, A.; Gall, C. Antioxidant and other biological activities of phenols from olives and olive oil. *Med. Res. Rev.* **2002**, *22*, 65–75.
(8) Visioli, F.; Romani, A.; Mulinacci, N.; Zarini, S.; Conte, D.; Vincieri, F. F.; Galli, C. Antioxidant and other biological activities of olive mill waste waters. *J. Agric. Food Chem.* **1999**, *47*, 3397–3401.
(9) Visioli, F.; Wolfram, R.; Richard, D.; Abdullah, M. I. C. B.; Crea, R. Olive Phenolics increase glutathione levels in healthy volunteers. *J. Agric. Food Chem.* **2009**, *57*, 1793–1796.
(10) Leger, C. L.; Carbonneau, M. A.; Michel, F.; Mas, E.; Monnier, L.; Cristol, J. P.; Descomps, B. A thromboxane effect of a hydroxytyrosol-rich olive oil wastewater extract in patients with uncomplicated type 1 diabetes. *Eur. J. Clin. Nutr.* **2005**, *59*, 727–730.
(11) Carluccio, M. A.; Siculella, L.; Ancora, M. A.; Massaro, M.; Scoditti, E.; Storelli, C.; Visioli, F.; Distante, A.; De Caterina, R. Olive oil and red wine antioxidant polyphenols inhibit endothelial activation: antiatherogenic properties of Mediterranean diet phytochemicals. *Arterioscler., Thromb., Vasc. Biol.* **2003**, *23*, 622–9.
(12) Calixto, J. B.; Campos, M. M.; Otuki, M. F.; Santos, A. R. Anti-inflammatory compounds of plant origin. Part II. Modulation of pro-inflammatory cytokines, chemokines and adhesion molecules. *Planta Med.* **2004**, *70*, 93–103.
(13) Bitler, C. M.; Viale, T. M.; Damaj, B.; Crea, R. Hydrolyzed olive vegetation water in mice has anti-inflammatory activity. *J. Nutr.* **2005**, *135*, 1475–1479.
(14) Demopoulos, C. A.; Pinckard, R. N.; Hanahan, D. J. Platelet-activating factor. Evidence for 1-O-alkyl-2-acetyl-sn-glyceryl-3-phosphorylcholine as the active component (a new class of lipid chemical mediators). *J. Biol. Chem.* **1979**, *254*, 9355–8.
(15) Prescott, S. M.; Zimmerman, G. A.; Stafforini, D. M.; McIntyre, T. M. Platelet-activating factor and related lipid mediators. *Annu. Rev. Biochem.* **2000**, *69*, 419–45.
(16) Demopoulos, C. A.; Karantonis, H. C.; Antonopoulou, S. Platelet activating factor - a molecular link between atherosclerosis theories. *Eur. J. Lipid Sci. Technol.* **2003**, *105*, 705–716.
(17) Karantonis, H. C.; Tsantila, N.; Stamatakis, G.; Samiotaki, M.; Panayotou, G.; Antonopoulou, S.; Demopoulos, C. A. Bioactive polar lipids in olive oil, pomace and waste byproducts. *J. Food Biochem.* **2008**, *32*, 443–459.
(18) Tsantila, N.; Karantonis, H. C.; Perrea, D. N.; Theocharis, S. E.; Iliopoulos, D. G.; Antonopoulou, S.; Demopoulos, C. A. Antithrombotic and antiatherosclerotic properties of olive oil and olive pomace polar extracts in rabbits. *Mediators Inflammation* **2007**, *2007*, 36204.
(19) Karantonis, H. C.; Antonopoulou, S.; Perrea, D. N.; Sokolis, D. P.; Theocharis, S. E.; Kavantzas, N.; Iliopoulos, D. G.; Demopoulos, C. A. In vivo antiatherogenic properties of olive oil and its constituent lipid classes in hyperlipidemic rabbits. *Nutr. Metab. Cardiovasc. Dis.* **2006**, *16*, 174–185.
(20) Harben, P. W. *The Industrial Mineral Handybook—A Guide to markets, specifications & prizes*, 4th ed.; Taylor, L., Ed.; Industrial Mineral Information: Worcester Park, Surrey, 2002; pp 1−412.
(21) Ilia, K. I.; Stamatakis, M. G.; Perraki, T. S. Mineralogy and technical properties of clayey diatomites from north and central Greece. *Cent. Eur. J. Geosci.*, in press.
(22) Bligh, E. G.; Dyer, W. J. A rapid method of total lipid extraction and purification. *Can. J. Biochem. Physiol.* **1959**, *37*, 911–917.
(23) Galanos, D. S.; Kapoulas, V. M. Isolation of polar lipids from triglyceride mixtures. *J. Lipid Res.* **1962**, *3*, 134–137.
(24) Obied, H. K.; Allen, M. S.; Bedgood, D. R., Jr; Prenzler, P. D.; Robards, K. Investigation of Australian olive mill waste for recovery of biophenols. *J. Agric. Food Chem.* **2005**, *53*, 9911–20.
(25) Karantonis, H. C.; Antonopoulou, S.; Demopoulos, C. A. Antithrombotic lipid minor constituents from vegetable oils. Comparison between olive oils and others. *J. Agric. Food Chem.* **2002**, *50*, 1150–1160.
(26) Singleton, V. L.; Rossi, J. A. Colorimetry of total phenolics with phosphomolybdic-phosphotungstic acid reagents. *Am. J. Enol. Vitic.* **1965**, *16*, 144–158.
(27) Mateos, R.; Espartero, J. L.; Trujillo, M.; Rios, J. J.; Leon-Camacho, M.; Alcudia, F.; Cert, A. Determination of phenols, flavones, and lignans in virgin olive oils by solid-phase extraction and high-performance liquid chromatography with diode array ultraviolet detection. *J. Agric. Food Chem.* **2001**, *49*, 2185–92.
(28) Mazza, G.; Fukumoto, L.; Delaquis, P.; Girard, B.; Ewert, B. Anthocyanins, phenolics, and color of Cabernet Franc, Merlot, and Pinot Noir wines from British Columbia. *J. Agric. Food Chem.* **1999**, *47*, 4009–17.
(29) Galanos, D. S.; Kapoulas, V. M. Preparation and analysis of lipid extracts from milk and other tissues. *Biochim. Biophys. Acta* **1965**, *98*, 278–292.
(30) Magalhaes, L. M.; Segundo, M. A.; Reis, S.; Lima, J. L. Methodological aspects about in vitro evaluation of antioxidant properties. *Anal. Chim. Acta* **2008**, *613*, 1–19.
(31) Santi, C. A.; Cortes, S.; D'Acqui, L. P.; Sparvoli, E.; Pushparaj, B. Reduction of organic pollutants in olive mill wastewater by using different mineral substrates as adsorbents. *Bioresour. Technol.* **2008**, *99*, 1945–1951.
(32) Al-Malah, K.; Azzam, M. O. J.; Abu-Lail, N. I. Olive mills effluent (OME) wastewater post-treatment using activated clay. *Sep. Purif. Technol.* **2000**, *20*, 225–234.
(33) Fan, G. J.; Kim, S.; Han, B. H.; Han, Y. N. Glyceroglycolipids, a novel class of platelet-activating factor antagonists from Kalimeris indica. *Phytochem. Lett.* **2008**, *1*, 207–210.
(34) Onal, M.; Sarikaya, Y.; Alemdaroglu, T.; Bozdogan, I. The effect of acid activation on some physicochemical properties of a bentonite. *Turk. J. Chem.* **2002**, *26*, 409–416.
(35) Heim, K. E.; Tagliaferro, A. R.; Bobilya, D. J. Flavonoid antioxidants: chemistry, metabolism and structure-activity relationships. *J. Nutr. Biochem.* **2002**, *13*, 572–584.

Received for review May 18, 2009. Revised manuscript received October 14, 2009. Accepted October 15, 2009. The present study was partially supported by the National Bank of Greece and the Special Account for Research Grants, University of Athens.